



iJRASET

International Journal For Research in
Applied Science and Engineering Technology



INTERNATIONAL JOURNAL FOR RESEARCH

IN APPLIED SCIENCE & ENGINEERING TECHNOLOGY

Volume: 12 Issue: IX Month of publication: September 2024

DOI: <https://doi.org/10.22214/ijraset.2024.64323>

www.ijraset.com

Call:  08813907089

E-mail ID: ijraset@gmail.com

Effect of Infill Pattern on Flexural Behaviour and Surface Roughness Behaviour of 3D Printed Poly Lactic Acid (PLA) Material

Preetish K S¹, Harish S²

¹M.Tech Scholar Department of Mechanical Engineering, Sri Siddhartha Institute of Technology, Tumkur – 572105

²Assistant Professor Department of Mechanical Engineering, Sri Siddhartha Institute of Technology, Tumkur – 572105

Abstract: This study aims to examine how the infill pattern affects the flexural behaviour of PLA objects that are 3D printed. Fused Deposition Modelling (FDM) was used to build polylactic acid (PLA) pieces at different infill patterns with a 100% infill density. Fourteen distinct infill patterns have been studied (Grid, Lines, Triangles, Tri-Hexagon, Cubic, Cubic Subdivision, Octet, Quarter Cubic, Concentric, Zig-Zag, Cross, Cross 3D, Gyroid, Lightning). Because of the increased strength of the strut connections in this pattern, the results demonstrated that the Tri-Hexagon infill pattern had the highest mechanical qualities, with 1088.24 MPa. Whereas Grid type infill pattern show minimum flexural strength of 296.79 MPa. There is a increase of 266.6% in flexural strength of Tri-Hexagon against Grid type infill pattern. This was due to the pattern's huge air gaps, which caused the pattern to fracture quickly during testing. Surface roughness of Zig-zag pattern shows the minimum value of $R_q = 4.94 \mu\text{m}$ and $R_z = 15.96 \mu\text{m}$. It can be concluded that the Tri-Hexagon infill pattern is quite promising when considering the construction time and the amount of filament used whereas Zig-zag pattern can be preferred if surface finish is the concern. The results of this study will assist researchers and manufacturing companies in selecting the right infill pattern, enabling the fabrication of FDM parts with high mechanical qualities and low production costs.

Keywords: Fused deposition modeling, 3D printing, Infill pattern, Flexural strength, Surface roughness

I. INTRODUCTION

Layer upon layer of material is added during additive manufacturing (AM) to construct three-dimensional (3D) objects for a wide range of industrial and other uses. A range of defence applications use AM, in contrast to standard production techniques that remove material until the desired part is created. Vehicle, aerospace, and medical industries, etc. Laminated Object Manufacturing (LOM), Selective Laser Sintering (SLS), Stereolithography (SLA), and other AM processes are only a few examples. Fused Deposition Modelling (FDM) is a prominent additive manufacturing process that is widely utilised globally [1-3]. The FDM process, which is ecologically benign and offers minimal maintenance and fabrication costs even for complicated products, is accessible in a wide range of materials [4]. G-code files are produced straight from STL-formatted CAD files. Using this method, pieces are made by putting material on top of material until the part takes on the desired shape. As seen in Fig. 1 [5], filament is heated to a semi-liquid state, and G-code regulates the nozzle's movement.

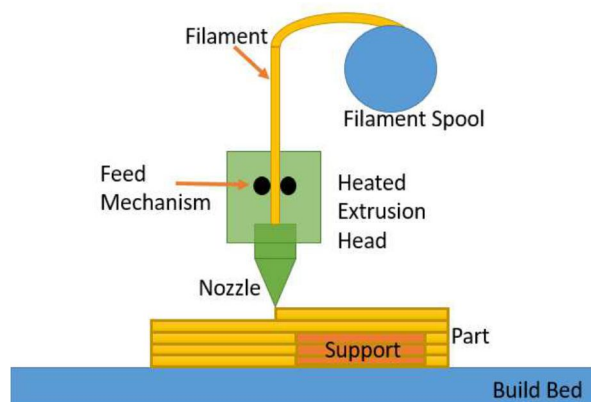


Fig. 1. Schematic diagram of FDM process

The component qualities and production efficiency in FDM are greatly influenced by a number of process variables. Important process parameters include layer thickness, raster angle, build orientation, infill density, printing speed, infill pattern, raster width, etc. Scientists are still at work. Find the ideal parameter configurations. Therefore, in order to determine the best process parameters and improve the mechanical qualities of the 3D printed PLA parts, a greater understanding of the FDM process is needed. One of the most important FDM process factors, infill pattern offers integrated support for the 3D print as every layer is constructed by the printer. As a result, many infill patterns have been studied by academics who worked on octagonal honeycomb patterns [1, 2], [6].

II. MATERIAL AND METHOD

Fig. 2 illustrates the use of 1.75 mm diameter commercial polylactic acid (PLA) filament as feedstock for a Advance - Hyrel 3D printer with a 0.4 mm diameter nozzle. All of the sample data were in STL format, which was converted into G-code and then sliced using Ultimaker cura software.

Ultimaker cura is a open-source software for slicers. Infill density, print speed, layer width, raster angle, build orientation, printing, and bed temperature have all been maintained while the infill pattern has been altered in this study. The infill patterns chosen for this investigation included Grid, Lines, Triangles, Tri-Hexagon, Cubic, Cubic Subdivision, Octet, Quarter Cubic, Concentric, Zig-Zag, Cross, Cross 3D, Gyroid, Lightning as shown in Fig.3.

The American Society for Testing and Materials (ASTM) D790 standard, depicted in Fig. 5, was followed in the fabrication of the parts. The process parameters listed in Table 1 were followed in the construction of the flexural test PLA samples (Fig. 6). For the three-point bending flexural test, rectangular cross-section specimens having dimensions $80 \times 10 \times 4$ mm were fabricated. Using an Instron 8872 universal testing equipment with a 25 kN load cell and a test speed of 1 mm/min at room temperature, the flexural strengths of the 3D printed PLA pieces were evaluated.

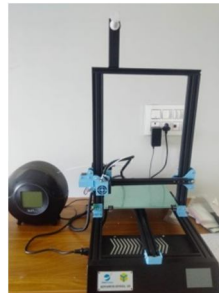


Fig. 2. Advance - Hyrel 3D printer

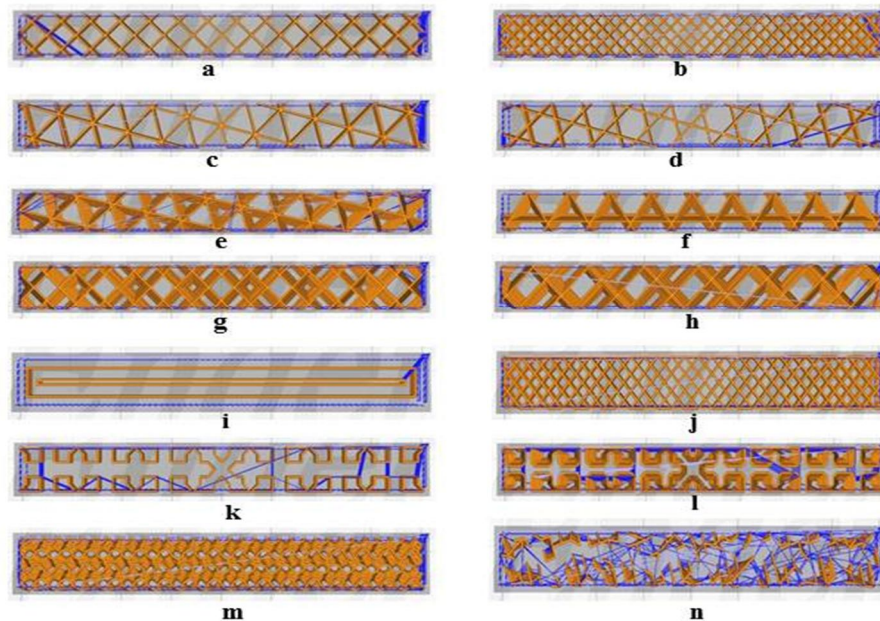


Fig. 3. Schematic diagram of infill pattern with infill density of 30%: a - Grid; b - Lines; c - Triangles; d - Tri-Hexagon; e - Cubic; f - Cubic Subdivision; g - Octet; h - Quarter Cubic; i - Concentric; j - Zig-Zag; k - Cross; l - Cross 3D; m - Gyroid; n - Lightning.

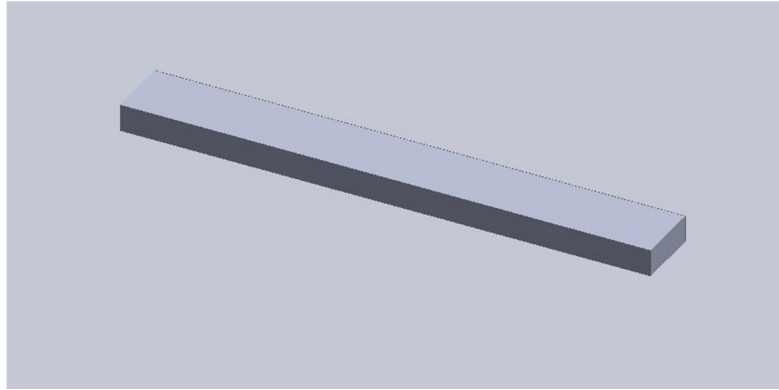


Fig. 4. Schematic diagram of CAD model of Flexural sample

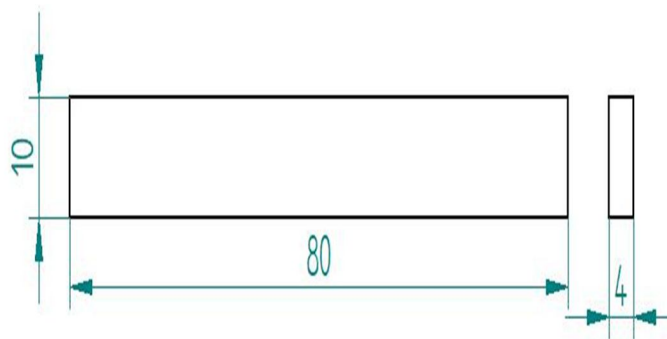


Fig. 5. Dimension details of flexural test specimen (dimensions in mm)

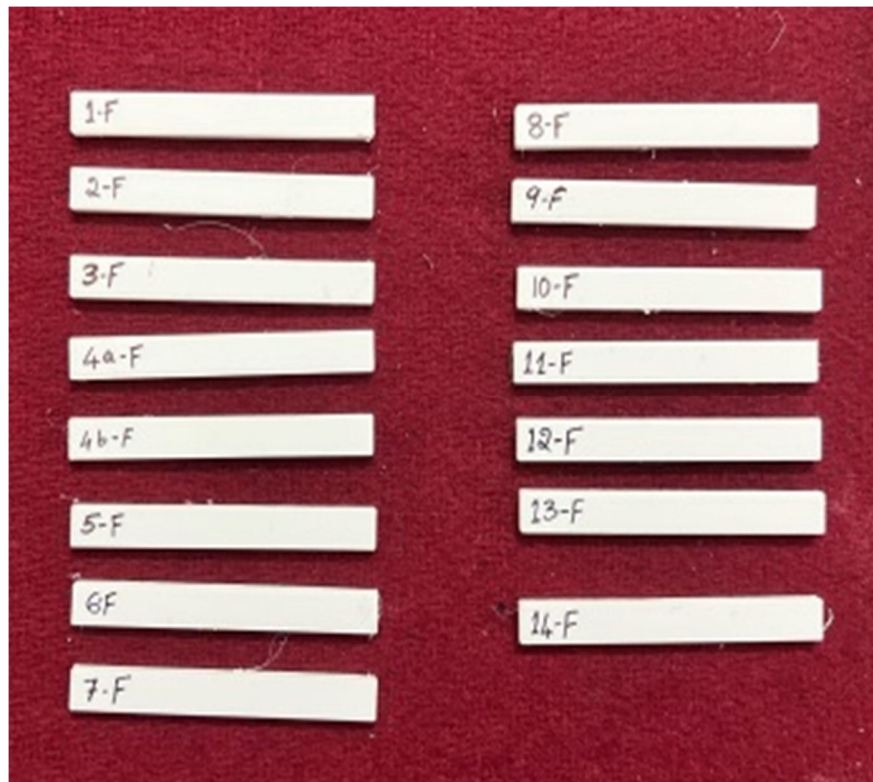


Fig. 6. Fabricated 3D printed PLA parts

III. SURFACE ROUGHNESS MEASUREMENT



Fig. 7: Surface Roughness Profilometer

Five sets of measurement conditions at most can be stored in the SJ-301 main unit. For every workpiece, different measuring circumstances can be chosen. By pressing key commands, the SJ-301's stored measuring conditions can be accessed and changed. Heat-insulated frame, ratchet stop, 0 – 25 mm range, 0.01 mm graduation, and ± 0.002 mm accuracy characterises the Mitutoyo 102 – 301 outside micrometre. The SurfTest SJ-310's flexibility and throughput increase productivity with its excellent precision (resolution of $0.002\mu\text{m}$ at a measuring range of $25\mu\text{m}$), quick measurement speed (max. 0.75 mm/s), choice of 11 interchangeable detector tips, and features like gear tooth surface detection.

IV. RESULTS AND DISCUSSION

The 3D printed samples were tested for three-point bending and surface roughness measurement were carried out and the results are tabulated as shown in Table 1. Infill pattern Tri-Hexagon is prepared with two infill density 20 % and 100 %. Results reveal that 100 % Infill density shows higher flexural strength. Therefore, all infill patterns were prepared with 100 % infill density.

Table 1: Flexural strength and Surface Roughness results

Sample ID	Infill Pattern type	Infill density (%)	Flexural Strength (N/mm^2)	Surface Roughness	
				R_q (μm)	R_z (μm)
1 - F	Grid	100	296.79	6.67	22.59
2 - F	Lines	100	840.91	5.98	20.73
3 - F	Triangles	100	544.12	5.20	16.69
4a - F	Tri-Hexagon (a)	100	1088.24	5.38	17.44
4b - F	Tri-Hexagon (b)	20	296.79	6.75	23.01
5 - F	Cubic	100	593.58	6.48	22.02
6 - F	Cubic Subdivision	100	692.52	6.17	19.99
7 - F	Octet	100	445.19	5.34	20.03
8 - F	Quarter Cubic	100	890.38	5.35	16.75
9 - F	Concentric	100	445.19	5.64	18.35
10 - F	Zig-Zag	100	544.12	4.94	15.96
11 - F	Cross	100	593.58	6.19	20.20
12 - F	Cross 3D	100	544.12	6.20	19.44
13 - F	Gyroid	100	494.65	6.67	22.59
14 - F	Lightning	100	544.12	5.98	20.73

Fig. 8 shows the picture of sample condition before and after the three-point bending test. All tests were conducted as per the standard and it can be observed that the fracture occurs in the gauge length.

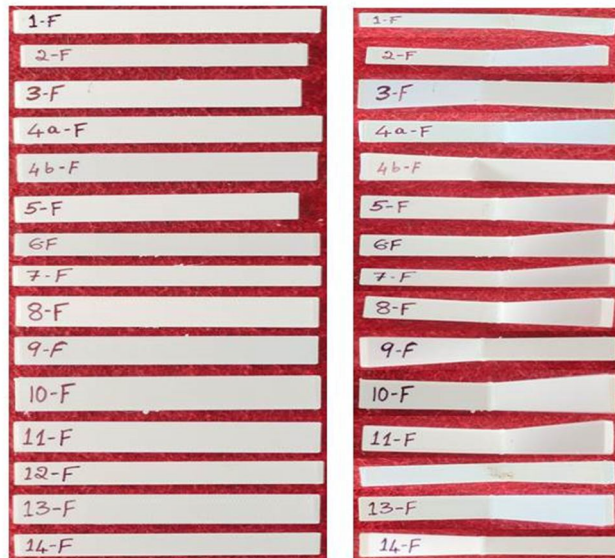


Fig. 8: Sample before and after the flexural test

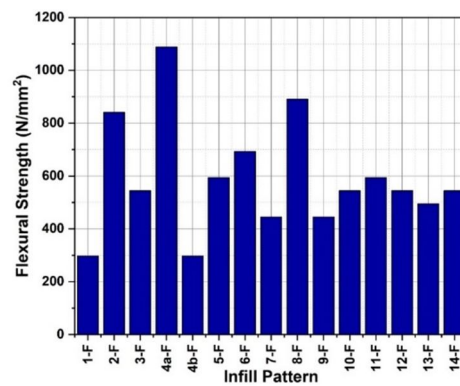


Fig. 9: Flexural strength for different infill patterns

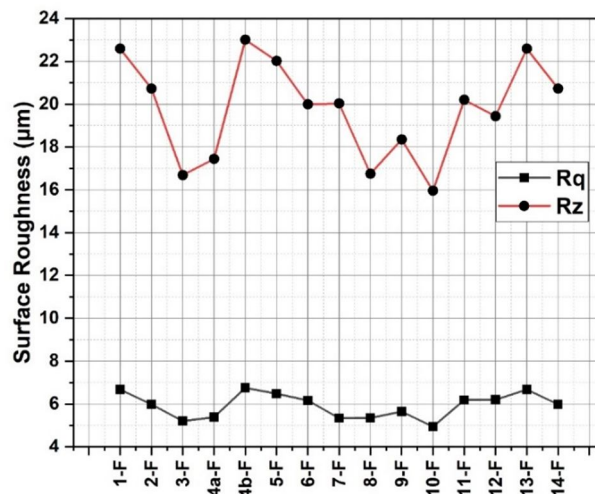


Fig. 10: Surface Roughness measurement for different infill patterns

Fig. 9 shows the flexural strength for different infill patterns. It is evident that Tri-Hexagon type infill pattern shows highest flexural strength of 1088.24 N/mm^2 whereas Grid type infill pattern shows the minimum flexural strength of 296.79 N/mm^2 . This is due to the effectiveness of adhesion between layers. Strong layer adhesion can enhance flexural strength significantly.

Fig. 10 shows the surface roughness measurement for different infill patterns. Zig-zag type infill pattern shows minimum surface roughness as 3D printed parts results in high roughness. This can be minimized by good layer adhesion which reduces issues like stringing or blobs, which can create rough spots.

V. CONCLUSION

Infill pattern and infill density had direct effects on the surface quality and mechanical properties of 3D-printed products. In the present work fourteen distinct infill patterns have been studied (Grid, Lines, Triangles, Tri-Hexagon, Cubic, Cubic Subdivision, Octet, Quarter Cubic, Concentric, Zig-Zag, Cross, Cross 3D, Gyroid, Lightning). The samples were 3D printed using Advance - Hyrel 3D printer and slicing was made using Ultimaker Cura software. Results show that Tri-Hexagon infill pattern had the highest mechanical qualities, with 1088.24 MPa . Whereas Grid type infill pattern show minimum flexural strength of 296.79 MPa . This is due to the effectiveness of adhesion between layers. Strong layer adhesion can enhance flexural strength significantly. Surface roughness of Zig-zag pattern shows the minimum value of $R_q = 4.94 \mu\text{m}$ and $R_z = 15.96 \mu\text{m}$. Surface roughness can be minimized by good layer adhesion which reduces issues like stringing or blobs, which can create rough spots.

VI. ACKNOWLEDGMENT

I would like to express my sincere gratitude to SRI SIDDHARTHA INSTITUTE OF TECHNOLOGY, TUMKUR for their invaluable support throughout my research.

REFERENCES

- [1] M. Altan, M. Eryildiz, B. Gumus, and Y. Kahraman, "Effects of process parameters on the quality of PLA products fabricated by fused deposition modeling (FDM): surface roughness and tensile strength", *Materials Testing*, vol. 60, no. 5, pp. 471–477, 2018.
- [2] R. Srinivasan, W. Ruban, A. Deepanraj, R. Bhuvanesh, and T. Bhuvanesh, "Effect on infill density on mechanical properties of PETG part fabricated by fused deposition modelling", *Materials Today: Proceedings*, vol. 27, part 2, pp. 1838–1842, 2020.
- [3] S. Bardiya, J. Jerald, and V. Satheeshkumar, "Effect of process parameters on the impact strength of fused filament fabricated (FFF) polylactic acid (PLA) parts", *Materials Today: Proceedings*, vol. 41, part 5, pp. 1103–1106, 2021.
- [4] A. Garg, A. Bhattacharya, and A. Batish, "On Surface Finish and Dimensional Accuracy of FDM Parts after Cold Vapor Treatment", *Materials and Manufacturing Processes*, vol. 31, no. 4, pp. 522–529, 2015.
- [5] A. Alafaghani, A. Qattawi, B. Alrawi, and A. Guzman, "Experimental Optimization of Fused Deposition Modelling Processing Parameters: A Design-for-Manufacturing Approach", *Procedia Manufacturing*, vol. 10, pp. 791–803, 2017.
- [6] R. Hedayati, M. Sadighi, M. Mohammadi-Aghdam, and A. A. Zadpoor, "Mechanical properties of additively manufactured octagonal honeycombs", *Materials science & engineering. C, Materials for biological applications*, vol. 69, pp. 1307–1317, 2016.



10.22214/IJRASET



45.98



IMPACT FACTOR:
7.129



IMPACT FACTOR:
7.429



INTERNATIONAL JOURNAL FOR RESEARCH

IN APPLIED SCIENCE & ENGINEERING TECHNOLOGY

Call : 08813907089  (24*7 Support on Whatsapp)